

SPACE HARMONIC CONTENT OF THE $2\pi/3$ ACCELERATOR STRUCTURE

By

Renée Hirel*

Internal Memorandum
Project M Report No. 270
June 1961

Project M
Stanford University
Stanford, California

* On leave from Laboratoire de l'Accelérateur Lineaire,
Orsay (Seine et Oise) France.

TABLE OF CONTENTS

| | Page |
|---|------|
| I. Introduction | 1 |
| Method I | 1 |
| Method II | 2 |
| II. Comparison of the two methods | 2 |
| III. Measurements | 9 |

I. INTRODUCTION

In a periodic structure with period L , the field distribution for a given mode can be expressed as

$$E_z = \sum_{n=-\infty}^{+\infty} a_n e^{-j\beta_n z} e^{j\omega t}$$

In a cavity formed by putting reflection terminations in symmetrical transverse plans it can be shown that

$$E_z = \sum_{n=-\infty}^{+\infty} 2a_n \cos \beta_n z e^{j\omega t}$$

Introducing¹ a dielectric or metallic bead on the axis of the cavity produces a perturbation of the resonant frequency of the cavity, which becomes $F + \Delta F$, where $\Delta F \propto E^2$.

Method I. If the resonant frequency is measured for different positions (z) of the bead, it is possible to plot a function ΔF , proportional to E^2 , versus z , and it is possible to carry out a Fourier analysis of the function

$$a_n = \frac{2}{3L} \int_0^{3L/2} E(z) \cos \beta_n z dz$$

For evaluating the most interesting space-harmonic coefficient from the accelerator point of view, $a_0^2/\Sigma a_n^2$, it is easier, instead of calculating all the coefficients $a_0, a_{-1}, a_{+1} \dots$ as is usually done, to calculate only

$$a_0 = \frac{2}{3L} \int_0^{3L/2} E(z) \cos \beta_0 z dz$$

1. W. J. Gallagher, "Measurement techniques for periodic structures," Project M Report No. 205, Stanford University, Stanford, California, November 1960.

and directly

$$\sum a_n^2 = \frac{1}{3L} \int_0^{3L/2} E^2(z) dz$$

because

$$E^2(z) = \sum_{nm} 4a_n a_m \cos \beta_n z \cos \beta_m z dz$$

$$\int_0^{3L/2} E^2(z) dz \neq 0, \text{ only if } n = m$$

and thus

$$\int_0^{3L/2} E^2(z) dz = 3L \sum a_n^2$$

Method II. The second method consists of studying the response of the perturbed cavity for each position of the bead at a frequency which is constant and down about 2 db from the unperturbed frequency of the cavity (in order to insure that the response of the perturbed cavity is proportional to E^2). And it is then also possible to carry out a Fourier analysis and to obtain a_0 , Σa_n^2 , and $a_0^2/\Sigma a_n^2$.

II. COMPARISON OF THE TWO METHODS

A difficulty common to both methods is that of obtaining symmetry of the curve $E^2(z)$ [plotted from $z = 0$ to $z = 3L$] about $z = 3L/2$. The two probes, generator and detector do not perturb in the same way, even though they are adjusted to have very little effect on the resonant frequency. This asymmetry can be compensated for by very carefully adjusting the tuning plugs (shown in Fig. 1).

Method I is much more accurate than Method II because of the accuracy with which the frequency can be measured. However, most of the error arises from the Fourier analysis itself. In order to be able to compare different results the curve is resolved into the same

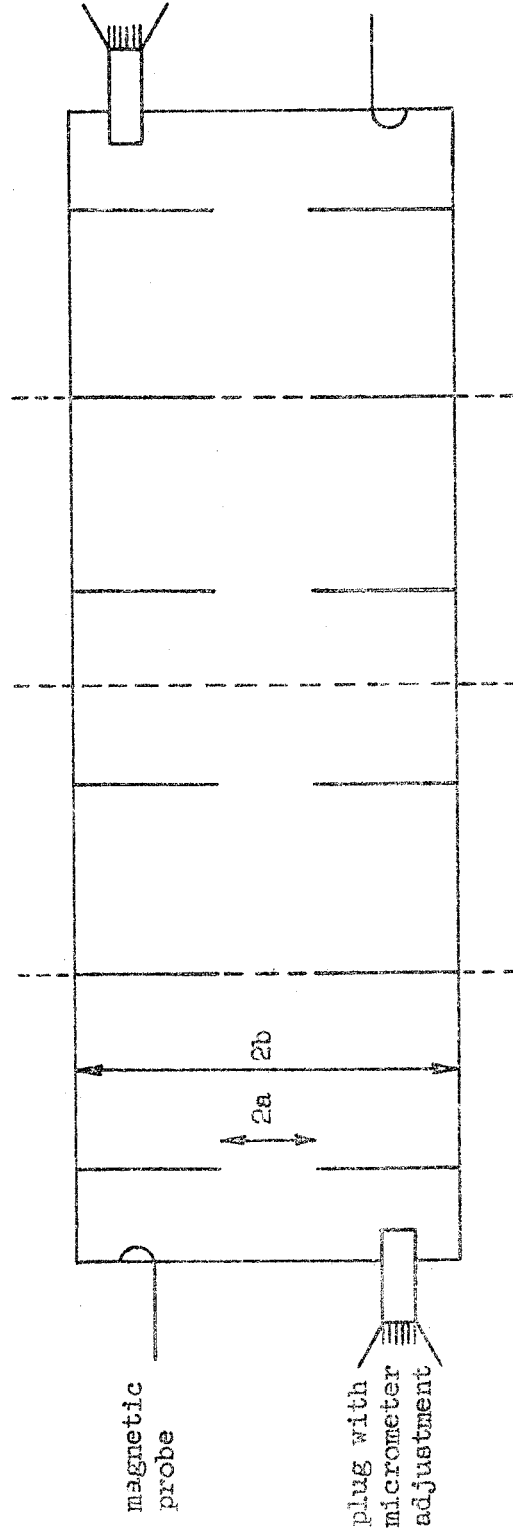


FIG. 1--Six-cavity structure with tuning plugs for obtaining the symmetry of the curve $E^2(z)$.

increments each time (n parts of $10.5/42 = .25$ cm).

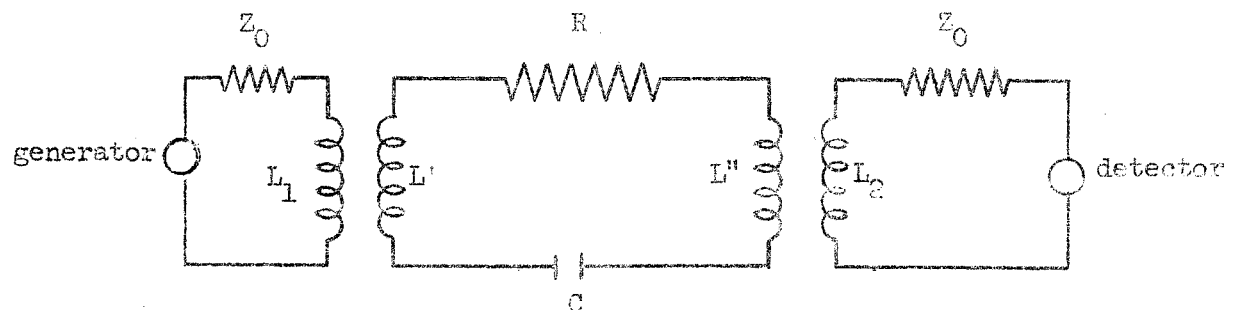
Method II is much easier to use than Method I (where the resonant frequency has to be adjusted for each position of the bead). In Method II, the curve of the response of the perturbed cavity for each position of the bead can even be registered with a recorder and can be obtained in a very short time. For these reasons the measurement previously done¹ have used Method II.

When the symmetry of the curve of $E^2(z)$ has been obtained for Method I by adjusting the tuning plugs, the curve of $E^2(z)$ obtained for Method II is still symmetrical (for the same position of the tuning plugs) for the 3-cavity case but not for the 6-cavity case (Fig. 2).

The curve of $E^2(z)$ for Method II can be considered as being obtained by taking the intersection with $F = F_0$ of the different resonance curves of the cavity corresponding to different positions of the bead (Fig. 3). It has been found that the amplitudes of the maxima of the resonance curves of the perturbed cavity vary with bead position, and especially for the 6-cavity case are different for $z = z_C$ and $z = z_E$ (the maximum being for the same frequency, however). In this case, it can be seen from Fig. 3 why for the same position of the tuning plugs the points C and E are symmetrical in the curve of $E^2(z)$ obtained by Method I, but not symmetrical in the curve of $E^2(z)$ obtained by Method II.

This change in the amplitudes of the maxima of the resonance curves of the cavity for different positions of the bead can be explained in terms of a variation in the coupling of the cavity to the generator and detector by some reflection on the bead (thus depending upon the position of the bead with respect to the end-walls).

Consider the equivalent low-frequency circuit of the generator-cavity-detector.



1. W. J. Gallagher, *ibid.*

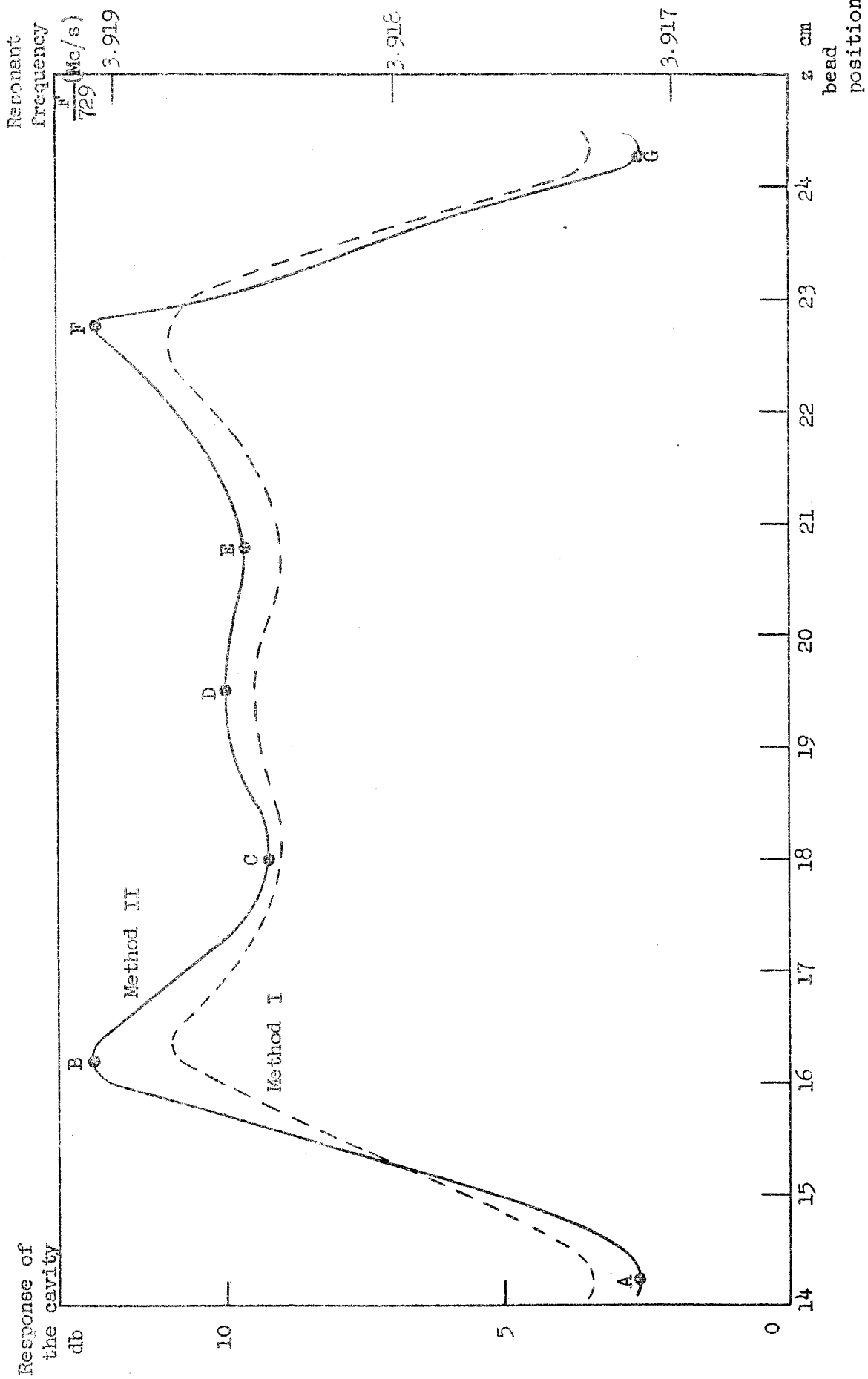


FIG. 2--Method II: Response of the cavity $F = F_0$ (down 2db from the unperturbed frequency) versus bead position.
 Method I: Resonance frequency of the cavity versus bead position.

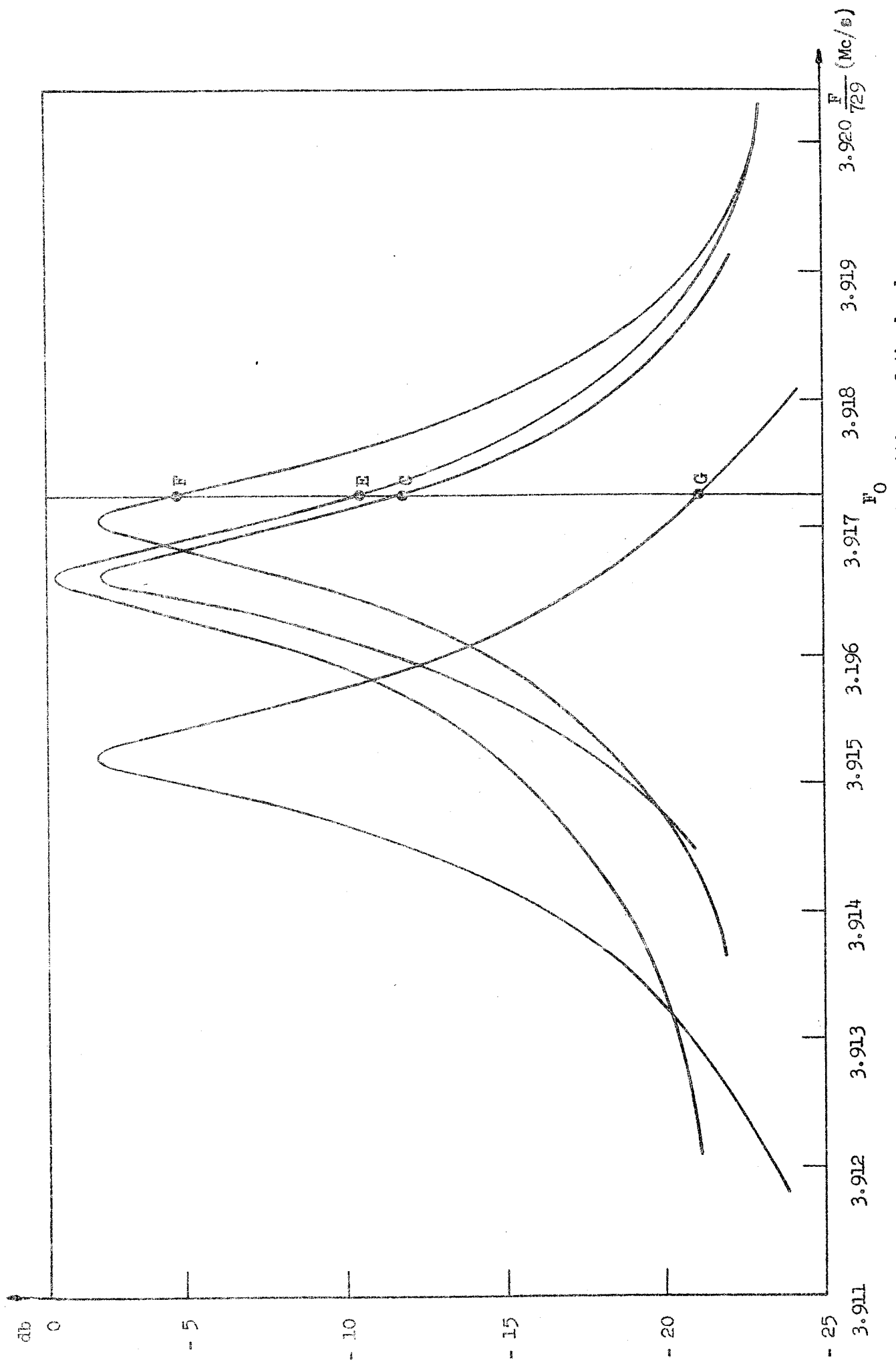


FIG. 3--Resonance - Curves of a 6-cavity structure for different positions of the bead.

Let the cavity be characterized by $L = L' + L''$, C , and R , where L and C vary with the bead position. The matched generator and detector are characterized by:

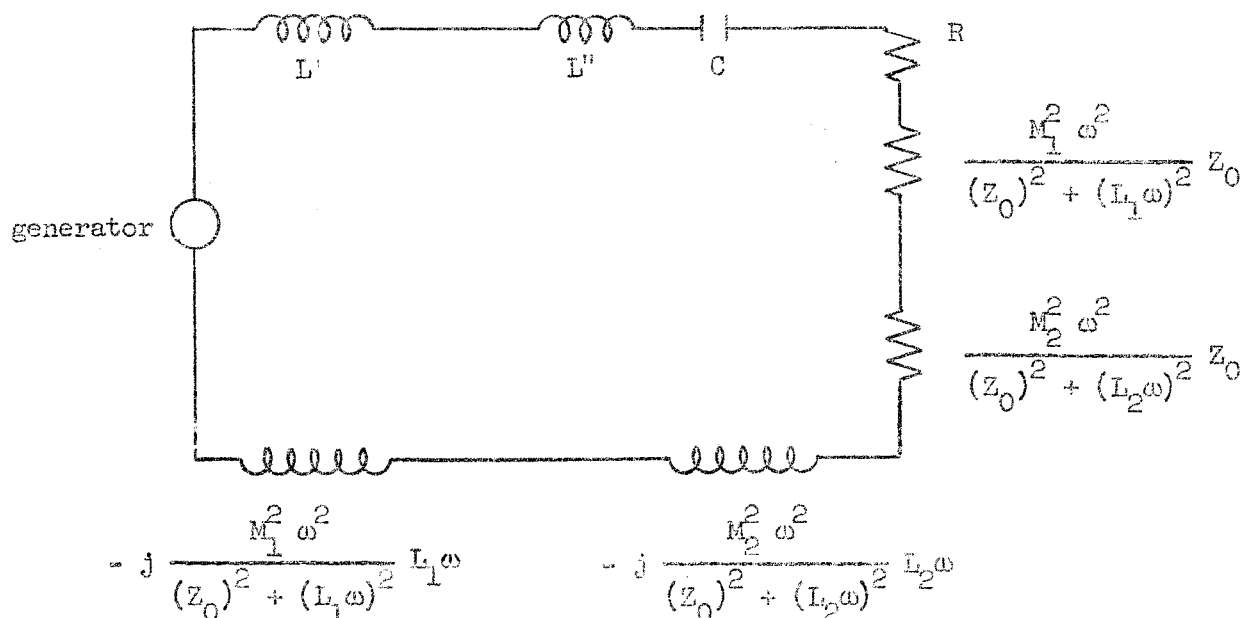
Z_0 = internal impedance

L_1, L_2 = self inductances of the loops

M_1, M_2 = mutual inductances between cavity and generator and detector

M_1 and M_2 are made very small by withdrawing the loops from the cavity until they have no effect on the resonant frequency; M_1 and M_2 are assumed to vary as a function of the bead position with respect to the end-wall.

This circuit can be transformed and represented as follows:



where

$$X_T = j \left(L \omega - \frac{1}{C \omega} \right) - j \frac{M_1^2 \omega^2}{(Z_0)^2 + (L_1 \omega)^2} L_1 \omega - j \frac{M_2^2 \omega^2}{(Z_0)^2 + (L_2 \omega)^2} L_2 \omega \quad (1)$$

$$R_T = R + \frac{M_1^2 \omega^2}{(Z_0)^2 + (L_1 \omega)^2} Z_0 + \frac{M_2^2 \omega^2}{(Z_0)^2 + (L_2 \omega)^2} Z_0 \quad (2)$$

A) From Eq. (1) it can be seen that, for a change in the bead position,

$$X_T \rightarrow X_T'$$

$$X_T' = j \left[(L + dL)\omega - \frac{1}{(C + dC)\omega} \right] - j \frac{(M_1 + dM_1)^2 \omega^2}{(Z_0)^2 + (L_1 \omega)^2} L_1 \omega - j \frac{(M_2 + dM_2)^2 \omega^2}{(Z_0)^2 + (L_2 \omega)^2} L_2 \omega.$$

For Method I, the value of ω_R which gives $X_T' = 0$ has to be found for each position of the bead. The tuning plugs are very carefully adjusted in order to make L_1 and L_2 small enough so that the second term and third term of X_T' are cancelled and

$$X_T' = j \left[(L + dL)\omega - \frac{1}{(C + dC)\omega} \right]$$

Here ω_R does not depend upon dM_1 and dM_2 and $(\omega_R)_C = (\omega_R)_E$ for either the 6- or 3-cavity cases. And it is known from experiment that the results of the Fourier analysis are the same for 6- and 3-cavity cases.

B) From Eq. (2) it can be seen that, because the maximum of the resonance curve of the cavity is proportional to v^2/R_T , it is important to know how R_T changes with the bead position for both the 3-cavity case and the 6-cavity case.

3-cavity case. The tuning plugs are still in the position where L_1 and $L_2 \simeq 0$. In the middle of the structure $z = 3L/2$, $M_1 = M_2$, and at any other points $M_1 + dM_1$ and $M_2 + dM_2$,

$$dR_T \simeq \frac{2M_1 \omega^2 Z_0}{Z_0^2} (dM_1 + dM_2)$$

For the points C and E which are at the same position with respect to the end-walls

$$(dM_1)_C = (dM_2)_E$$

$$(dM_2)_C = (dM_1)_E$$

thus

$$(dR_T)_C = (dR_T)_E$$

and the maxima of the resonance curves for C and E are the same.

6-cavity case. The tuning plugs are still in the position where L_1 and $L_2 \approx 0$. For $z = 3L/2$, $M_1 \neq M_2$ because the generator and detector are not the same distance from this point. For any other point $M_1 + dM_1$ and $M_2 + dM_2$,

$$dR_T \approx \frac{2\omega^2 Z_0}{Z_0^2} \left(M_1 dM_1 + M_2 dM_2 \right)$$

For the points C and E which are not at the same position with respect to the end-walls,

$$(dM_1)_C \neq (dM_2)_E$$

$$(dM_2)_C \neq (dM_1)_E$$

thus

$$(dR_T)_C \neq (dR_T)_E$$

and the maxima of the resonance curves for C and E are not the same (Fig. 3).

III. MEASUREMENTS

1. Method I has been used throughout all these measurements because it is more accurate and gives the same result for the 3-cavity and 6-cavity cases.

2. A significant error can arise if the curve is not perfectly symmetrical even if the asymmetry is very small. Thus the adjustment of the tuning plug has to be done very carefully.

3. The value of the space-harmonic coefficient $a_0^2/\lambda a_n^2$ for a given set of cavity cups has to be corrected when the resonant frequency is not exactly at 2856 Mc/s. Some additional measurements have to be done to determine more precisely the value of this correction.

4. Measurements of space-harmonic coefficients have been done here for the $2\pi/3$ mode at about 2856 Mc/s resonant frequency, on different sets of cavity cups with different disk thicknesses ($t = .060$ in., $t = .120$ in., $t = .230$ in.), and with different group velocity in order to evaluate the change of the space-harmonic coefficients with disk thickness and to determine if it seems promising, from this point of view, to use thin disks in the accelerator structure (shown in Fig. 4).

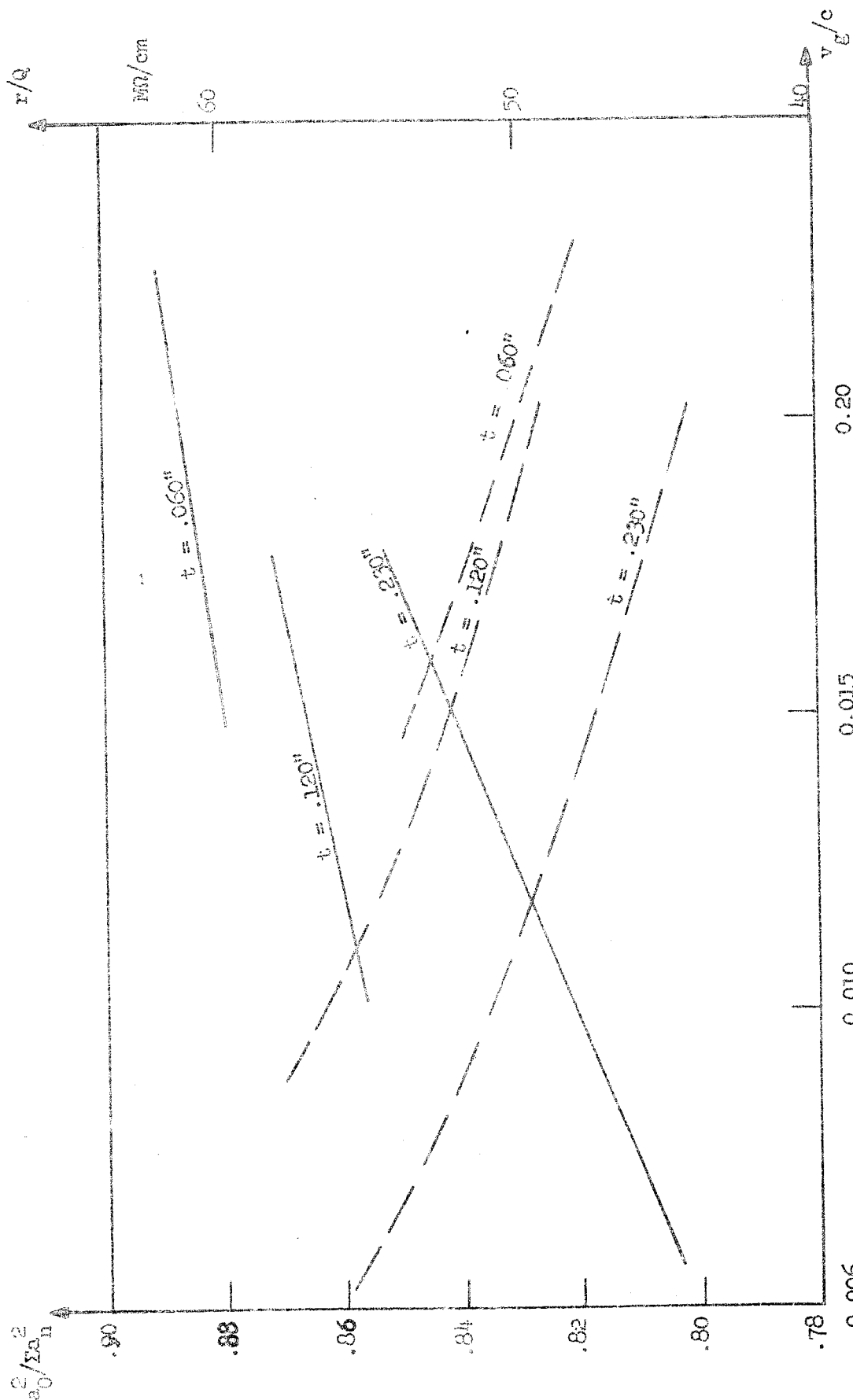


FIG. 4. $\frac{v_0^2}{v_g^2}$ vs $\frac{r}{q}$ for different disk thickness. $\frac{r}{q}$ versus $\frac{v_0^2}{v_g^2}$ for different disk thickness.